Emergent criticality and universality class of the finite-temperature charge-density-wave transition in lattice Bose gases within optical cavities

Liang He[*]

Guangdong Provincial Key Laboratory of Quantum Engineering and Quantum Materials, SPTE, South China Normal University, Guangzhou 510006, China

Su Yi[†]

CAS Key Laboratory of Theoretical Physics, Institute of Theoretical Physics, Chinese Academy of Sciences, Beijing 100190, China and School of Physical Sciences and CAS Center for Excellence in Topological Quantum Computation, University of Chinese Academy of Sciences, Beijing 100049, China

We investigate the finite-temperature charge-density-wave (CDW) transition of lattice Bose gases within optical cavities in the deep Mott-insulator limit. We find a new critical regime emerges at a temperature around one-half of the on-site interaction energy, where the first-order CDW transition at low temperatures terminates at a critical point and changes to a second-order one. By directly calculating the critical exponents and constructing the effective theory in the corresponding critical regime, we find the emergent criticality belongs to the five-dimensional Ising universality class. Direct experimental observation of the emergent criticality can be readily performed by current experimental setups operated in the temperature regime around half the on-site interaction energy.

I. INTRODUCTION

Long-range interactions can give rise to rich exotic structures and phases of matter, such as charge- and spin-density waves, supersolids, spin glasses, etc. Moreover, on the fundamental level, the long-range characteristic of interactions can play the same crucial role as symmetries and spatial dimensions of physical systems in determining their universal physical behavior in the critical regime of their continuous phase transitions [1,2]. In the context of ultracold atoms, various long-range interacting systems, ranging from ultracold gases with large magnetic or electric dipole moments [3,4], to atoms in Rydberg states [5], to ultracold gases in cavities with cavity-photon-mediated interactions [6–8], have been realized in experiments [3–8], making them powerful platforms to explore the fundamental behavior characteristic of long-range interactions.

A case in point is Bose gases in two-dimensional (2D) square optical lattices within optical cavities, which feature distinct *infinite*-long-range (ILR) interactions that are mediated by the cavity photons [8]. Recent experimental and theoretical investigations [8–17] have shown that at low temperatures this system can support rich phases and phase transitions attributed to its long-range interaction, such as supersolids, charge-density waves (CDWs), etc. In particular, by tuning the relative strength between the short-range on-site interaction and the ILR one in the deep Mott-insulator

regime, a new phase transition characteristic of a first-order one between the $\mathbb{Z}_2$-symmetric homogeneous Mott-insulator and the spontaneous $\mathbb{Z}_2$-symmetry-breaking CDW phase was observed in experiments [8]. Noticing that current experiments are mostly operated at a temperature scale that is much lower than all other energy scales in the system, it is intriguing to expect that at the evenly matched temperature scale, due to the interplay among short-range on-site interactions, ILR interactions, and thermal fluctuations, a completely different scenario for the CDW transition could arise. This thus raises the fundamental question of whether criticalities for the CDW transition, the existence of which is excluded at low temperatures in the first-order transition scenario, could emerge and bear the characteristic of the ILR interaction.

In this paper, we address the above question by establishing the complete finite-temperature phase diagram of the system in the deep Mott-insulator limit at unit filling [see Fig. 1(a)] and investigating the emergent critical scaling behavior of the system [see Figs. 2 and Figs. 3]. More specifically, we find the following.

(i) An emergent critical regime consists of a new critical point and second-order CDW transitions. At low temperatures, our calculations clearly show that the CDW transition is a first-order phase transition, i.e., the CDW order parameter $\bar{\phi}$ assumes a finite jump $\Delta\bar{\phi}$ when the transition boundary is crossed [see Figs. 1(a) and 1(b)], which corroborates observations in experiments [8]. When the temperature is increased, the jump of the CDW order parameter $\Delta\bar{\phi}$ decreases and finally vanishes at a critical point with its temperature $T_{\mathrm{CP}} = 0.39 U_s/k_B$ [U_s and k_B are the on-site energy strength and the Boltzmann constant, respectively; see Figs. 1(a) and 2]. Above

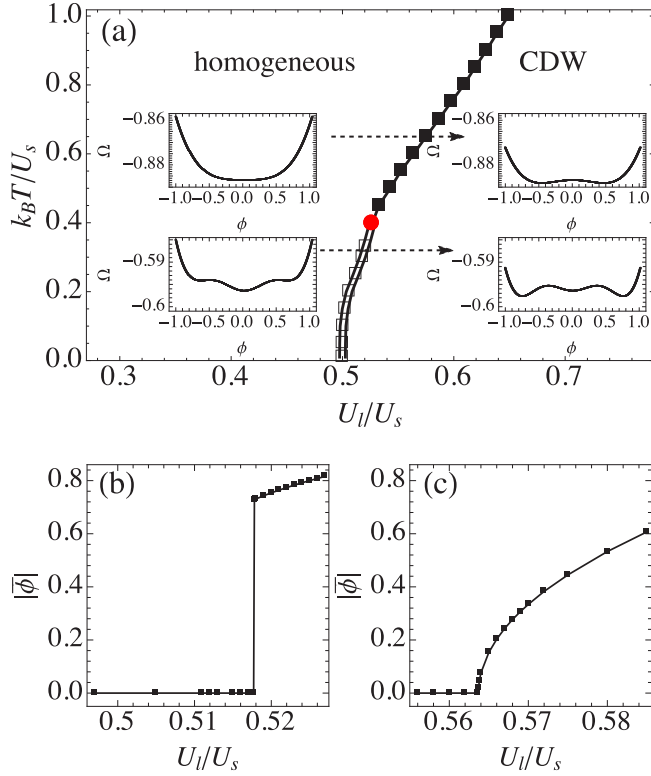[*]liang.he@scnu.edu.cn
[†]syi@itp.ac.cn

FIG. 1. (a) Finite-temperature phase diagram of lattice Bose gases within optical cavities in the deep Mott-insulator limit at unit filling. In the weak ILR interaction strength U_l regime the system is in the homogeneous phase, while in the strong ILR interaction regime, the system is in the CDW phase, where the system's density distribution assumes the checkerboard pattern. At low temperatures, the CDW transition between the homogeneous phase and the CDW phase upon tuning ILR interaction strength U_l is a first-order phase transition (marked by open squares and a double solid curve). At high temperatures, the first-order transition boundary terminates at a critical point (marked by the filled red disk) with temperature $T_{CP} = 0.396$ (in the unit of U_s/k_B, with an error less than 10^{-3}). Above the critical point, i.e., $T > T_{CP}$, the CDW transition becomes a second-order one (marked by solid squares and a solid curve). The insets in the phase diagram show the dependence of Ω on the CDW order-parameter field ϕ in four typical scenarios, namely, the homogeneous phase above (below) T_{CP} [the upper-left (lower-left) inset] and the CDW phase above (below) T_{CP} [the upper-right (lower-right) inset]. (b) The ILR interaction strength U_l dependence of the CDW order parameter $|\bar{\phi}|$ [lower dashed arrow in (a)] at a temperature below T_{CP} with $k_B T = 0.3 U_s$, showing the first-order transition upon increasing U_l. (c) The ILR interaction strength U_l dependence of the CDW order parameter $|\bar{\phi}|$ [upper dashed arrow in (a)] at a temperature above T_{CP} with $k_B T = 0.6 U_s$, showing the second-order transition upon increasing U_l. See text for more details.

the critical point, the CDW transition becomes a second-order transition, where the CDW order parameter changes continuously when crossing the transition boundary [see Figs. 1(a) and 1(c)].

(ii) The universality class of the emergent criticality belongs to the five-dimensional (5D) Ising universality class. The CDW order-parameter jump $\Delta\bar{\phi}$ along the first-order CDW transition boundary assumes a power-law scaling with
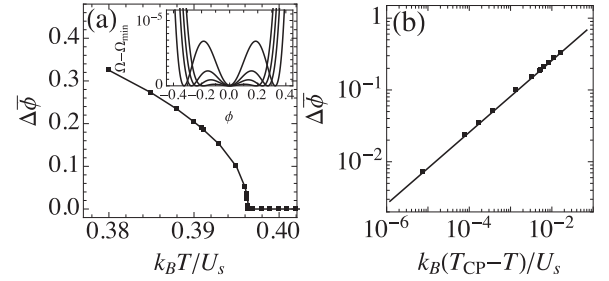

FIG. 2. (a) Temperature dependence of $\Delta\bar{\phi}$ along the first-order CDW transition boundary. Upon increasing T from the low-temperature regime with $T < T_{CP}$, $\Delta\bar{\phi}$ continuously decreases to zero at the temperature of the critical point $T_{CP} = 0.396 U_s/k_B$. The inset shows ϕ dependence of Ω at four different temperatures. The curves with their double well located from outer position to inner position correspond to $k_B T/U_s = 0.380, 0.385, 0.388, 0.391$, respectively. Ω_{min} denotes the minimum value of Ω for each curve. (b) Linear fit to the data points in (a) near the critical point with $T < T_{CP}$ on the double logarithmic scale, showing clearly a power-law dependence of $\Delta\bar{\phi}$ on $T_{CP} - T$, i.e., $\Delta\bar{\phi} \propto (T_{CP} - T)^\alpha$ with $\alpha = 0.500$. The solid line correspond to the best power-law fit $\Delta\bar{\phi} \propto (T_{CP} - T)^{0.500}$ to the data points in the plot. See text for more details.

respect to the temperature change near the critical point, i.e., $\Delta\bar{\phi} \propto (T_{CP} - T)^{0.5}$ (see Fig. 2). Moreover, the CDW order parameter also shows the same power-law scaling near the second-order CDW transition boundary, i.e., $|\bar{\phi}| \propto (T_c - T)^{0.5}$ with T_c being the critical temperature at the second-order transition boundary (see Fig. 3). Analyses of the effective theory in the critical regime [see Eqs. (4) and (5)] show this critical scaling behavior of this low dimensional 2D system belong to the universality class of short-range interacting systems with a much higher spatial dimension, i.e., the 5D Ising universality class. This clearly shows that the criticality of the system is strongly influenced by and thus bears the long-range characteristic of its interactions. Moreover, as far as we know, this also establishes lattice Bose gases in optical cavities as the first type of realistic physical system that accommodates
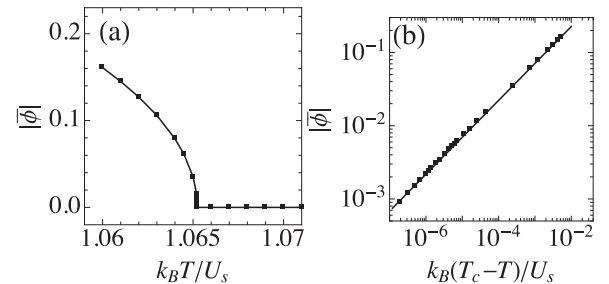

FIG. 3. (a) Temperature dependence of the CDW order parameter $|\bar{\phi}|$ at a fixed ILR interaction strength with $U_l/U_s = 0.66$. Upon increasing the temperature, $|\bar{\phi}|$ continuously decreases to zero at the critical temperature T_c ($k_B T_c/U_s = 1.065$) of the second-order CDW transition point. (b) Linear fit to the data points in (a) with $T < T_c$ on the double logarithmic scale, showing clearly a power-law dependence of $|\bar{\phi}|$ on $T_c - T$, i.e., $|\bar{\phi}| \propto (T_c - T)^\alpha$ with $\alpha = 0.504$. The solid line corresponds to the best power-law fit $|\bar{\phi}| \propto (T_c - T)^{0.504}$ to the data points in the plot. See text for more details.

exact physical manifestations of the largely academic 5D Ising universality class [18].

II. MODEL IN THE DEEP MOTT-INSULATOR LIMIT

For Bose gases in optical lattices located inside optical cavities, besides the conventional on-site interaction, the strong coupling between cavity photons and bosonic atoms can result in an effective ILR interaction for Bose gases [7,8]. Their physics in a wide range of the parameter space can be captured by the ILR interacting Bose-Hubbard model (see [8] or Appendix A for derivation details of this model), the Hamiltonian of which consists of a conventional hopping part and an interaction part. In this paper, we focus on the physics in the deep Mott-insulator limit, where the hopping amplitude is negligibly small, hence the system is described by the interaction part alone. In this limit, its Hamiltonian reads

$$\hat{H} = \frac{U_s}{2} \sum_{i,\sigma} \hat{n}_{i,\sigma}(\hat{n}_{i,\sigma}-1) - \frac{U_l}{L}\left(\sum_{i=1}^{L/2} \hat{n}_{i,e} - \sum_{i=1}^{L/2} \hat{n}_{i,o}\right)^2. \quad (1)$$

Here, the first term describes the conventional onsite interaction with its strength characterized by U_s. The second term describes the ILR interaction mediated by photons in the cavity [7,8] with its strength characterized by U_l. Moreover, in order to restore the conventional thermodynamical limit, U_l is further rescaled by the total number of lattice sites L in this term according to the Kac prescription [20]. Here, we consider the 2D square-lattice case which is the same as the experimental setup in Ref. [8], and refer to its two interpenetrating square sublattices as "even" (e) and "odd" (o) lattice, respectively. $\hat{n}_{i,\sigma}$ is the particle number operator that counts the number of atoms at site i on the sublattice σ, with $\sigma = e, o$. We remark here that although to be concrete we base our discussion on the 2D square lattice which is most relevant for the current experimental setups [8] the results to be presented in the following generally hold true for generic bipartite lattices.

From the Hamiltonian (1), we see that at fixed integer filling the short-range on-site interaction term favors a conventional Mott-insulator phase where the particle density is homogeneously distributed over the lattice, while the ILR interaction term favors a CDW phase with a checkerboard pattern where particle densities on the even and odd checkerboard sublattice are different, thus breaking the $\mathbb{Z}_2$ symmetry between the two sublattices [7]. The competition between these two types of interactions, hence two energy scales, gives rise to a phase transition associated with the $\mathbb{Z}_2$-symmetry breaking in the deep Mott-insulator limit as observed in experiments focusing at fixed low temperatures [8]. Taking into account the energy scale set by the temperature, one would expect the competition among these three energy scales could give rise to new physics beyond the one in the low-temperature regime. Indeed, as we shall see in the following, when the energy scale associated with the temperature can match the two other energy scales in the system, new criticalities that are dominated by the ILR interaction emerge.

III. EMERGENT CRITICALITY FOR THE CDW TRANSITION AT INTERMEDIATE-TEMPERATURE SCALES

Before discussing the main results, let us briefly outline the major method we used in our calculations. To investigate the finite-temperature phase transition between the CDW and the homogeneous phase (at low temperatures this corresponds to the homogeneous Mott insulator), we introduce the CDW order-parameter field ϕ into the quantum grand partition function Z of the system via the standard Hubbard-Stratonovich transformation and reformulate the grand partition function Z in terms of the ϕ field (see Appendix B), the explicit form of which reads

$$Z = \sqrt{\frac{\beta U_l L}{\pi}} \int_{-\infty}^{+\infty} d\phi \, e^{-\beta L \Omega_{\{\beta,\mu,U_s,U_l\}}(\phi)} \quad (2)$$

with

$$\Omega_{\{\beta,\mu,U_s,U_l\}}(\phi)$$
$$\equiv U_l\phi^2 - \frac{1}{2\beta} \sum_{\eta=\pm1} \ln\left[\sum_{n=0}^{+\infty} e^{-\beta[\frac{U_s}{2}n(n-1)-\mu n+2\eta U_l n\phi]}\right]. \quad (3)$$

Here, μ is the chemical potential and $\beta = (k_B T)^{-1}$ with k_B being the Boltzmann constant and T being the temperature. From Eq. (2), we notice that in the Mott-insulator limit where the hopping can be neglected the partition function of the system assumes a classical form, therefore the CDW transition in this limit is a classical transition. The transition from the homogenous phase to the CDW is characterized by the appearance of the nonzero expectation value of ϕ, i.e., CDW order parameter $\bar{\phi} \equiv \langle \phi \rangle = \langle \sum_{i=1}^{L/2} \hat{n}_{i,e} - \sum_{i=1}^{L/2} \hat{n}_{i,o}\rangle/L$ (see Appendix B). In the thermodynamic limit $L \to \infty$, the integral with respect to ϕ in Eq. (2) is given exactly by its saddle-point integration. Therefore, in the thermodynamic limit, $Z = (\sqrt{\beta U_l L/\pi}) \exp(-\beta L \min[\Omega_{\{\beta,\mu,U_s,U_l\}}(\phi)])$ and the CDW order parameter $\bar{\phi}$ is given by the value of ϕ that minimizes $\Omega_{\{\beta,\mu,U_s,U_l\}}(\phi)$. The summation in Eq. (3) cannot be performed analytically; however, it can be numerically calculated at a sufficiently high accuracy with a large enough cutoff on n. This enables us to map out the complete finite-temperature phase diagram as we shall now discuss.

At unit filling, the finite-temperature phase diagram is shown in Fig. 1(a). In the low-temperature regime (compared to half of the on-site energy), the transition from the homogenous phase to the CDW phase is a first-order transition, where the CDW order parameter shows a finite jump $\Delta\bar{\phi}$ when the system parameter is tuned across the transition boundary [see Fig. 1(b)]. This corroborates the findings in experiments where hysteretic behavior of the first-order CDW transition was observed in the low-temperature regime [8]. The first-order transition behavior can be traced back to the structure of the function $\Omega_{\{\beta,\mu,U_s,U_l\}}(\phi)$: For the homogeneous phase, $\Omega_{\{\beta,\mu,U_s,U_l\}}(\phi)$ has two types of minima, with one type of minimum located at $\phi = 0$ which is global and the other type located at $\pm\phi^*$, with $|\phi^*| \neq 0$ which is local [see lower-left inset in Fig. 1(a)]. When system parameters are tuned to approach the first-order transition boundary the difference in the Ω value between these two types of minima decreases. At

the first-order transition boundary, Ω assumes the same value at these two types of minima. After the system parameter enters the CDW regime, minima at $\pm\phi^*$ become the global minima [see lower-right inset in Fig. 1(a)], giving rise to the finite jump in the CDW order as shown in Fig. 1(b).

When the temperature is increased in the low-temperature regime, the order-parameter jump $\Delta\bar{\phi}$ at the first-order transition boundary decreases and finally vanishes at a critical point as shown by the red dot in Fig. 1(a) with its temperature $T_{\mathrm{CP}} = 0.396 U_s/k_B$. The emergence of the critical point can be traced back to the change of locations of the minima of Ω along the first-order transition boundary as shown in the inset of Fig. 2(a), where $|\phi^*|$ approaches zero when the temperature is increased.

Above the critical point, the CDW transition becomes a second-order phase transition, where the CDW order parameter changes continuously when system parameters are tuned across the transition boundary as shown in Fig. 1(c). The second-order transition behavior can also be traced back to the structure of the function $\Omega_{\{\beta,\mu,U_s,U_l\}}(\phi)$: On the homogeneous phase side of the transition, $\Omega_{\{\beta,\mu,U_s,U_l\}}(\phi)$ has only one global minimum located at $\phi = 0$ [see upper-left inset in Fig. 1(a)]. When the system parameters are tuned across the second-order transition boundary, this minimum continuously changes to a maximum, and two new minima emerging at $0^{\pm}$ at the same time. These two nonzero minima are continuously moving far away from $\phi = 0$ as system parameters are further tuned into a deeper CDW parameter regime [see upper-right inset in Fig. 1(a) and Fig. 1(c)].

The emergence of the critical point and the second-order CDW transition in fact gives rise to a new critical regime that is absent at low temperatures where the CDW transition is a first-order transition. Indeed, as we shall see in the following, in the vicinity of the critical point and the second-order transition, both the order-parameter jump $\Delta\bar{\phi}$ of the *first-order* transition and the order parameter $\bar{\phi}$ manifest critical power-law scaling that is dominated by the long-range interaction of the system.

IV. CRITICAL SCALING AND UNIVERSALITY CLASS OF CDW TRANSITION AT INTERMEDIATE TEMPERATURES

At low temperatures, the CDW order changes its value abruptly by $\Delta\bar{\phi}$ when system parameters, for instance, U_l, are tuned across the first-order transition boundary. Therefore, the CDW order parameter $\bar{\phi}$ itself does not show any critical power-law scaling. However, as we can see from Fig. 2(a), where numerical results of the temperature dependence of the order parameter jump $\Delta\bar{\phi}$ are shown, $\Delta\bar{\phi}$ decreases continuously upon increasing the temperature and finally vanishes at the critical point. This thus gives rise to the possible existence of the critical power scaling concerning the order-parameter jump $\Delta\bar{\phi}$ near the critical point. Indeed, as shown in Fig. 2(b), a power-law fit to the temperature dependence of $\Delta\bar{\phi}$ in the vicinity of the critical point T_{CP} clearly shows a critical scaling $\Delta\bar{\phi} \propto (T_{\mathrm{CP}} - T)^{0.500}$.

Above the critical point, i.e., $T > T_{\mathrm{CP}}$, the CDW transition becomes a second-order one, where CDW order changes continuously when system parameters are tuned across the transition boundary. Thus, one naturally expects the CDW

order $\bar{\phi}$ shows critical scaling near the second-order transition boundary. Indeed, as we can see from Fig. 3, where numerical results of the temperature dependence of CDW order parameter $|\bar{\phi}|$ at a fixed U_l are shown, a critical scaling $|\bar{\phi}| \propto (T_c - T)^{0.504}$ can be clearly observed [see Fig. 3(b)].

Interestingly, the numerical values for these two critical exponents, i.e., the one that governs the scaling of $\Delta\bar{\phi}$, which assumes the value of 0.500, and the other one that governs the scaling of $|\bar{\phi}|$, which assumes the value of 0.504, respectively, are remarkably close to each other. This thus strongly suggests these two critical scaling behaviors are related to each other on the fundamental level by the same effective theory in their respective critical regime. Indeed, both scalings can be determined via the same effective theory within the Ginzburg-Landau (GL) framework, as we shall now discuss.

In the critical regime, the CDW order parameter is small enough to allow a systematic expansion of the system's free energy F with respect to its CDW order parameter $\bar{\phi}$. The $\mathbb{Z}_2$ symmetry of the system determines the allowed terms in the expansion, the explicit form of which up to the sixth order in $\bar{\phi}$ reads

$$F = \tfrac{1}{2}r\bar{\phi}^2 + \tfrac{1}{4}u_4\bar{\phi}^4 + \tfrac{1}{6}u_6\bar{\phi}^6, \tag{4}$$

with r, u_4, and u_6 being the GL coefficients. To describe the first-order transition, one further assumes that r depends on temperature linearly, i.e., $r = a(T_{\mathrm{CP}} - T)$ where a is a positive coefficient, and $u_{4,6}$ are temperature independent coefficients with u_4 assumed to be negative for $T < T_{\mathrm{CP}}$ and u_6 being always positive in order to stabilize the whole system. To describe the second-order transition above the critical point, one assumes that r depends on temperature linearly, i.e., $r = a(T - T_c)$ with T_c being the critical temperature of the second-order CDW transition, and u_4 is positive, hence the sixth-order term in Eq. (4) is thus irrelevant in this case. By analyzing the saddle points of F in these two cases, we can obtain that, for the first-order transition, the CDW order-parameter jump $\Delta\bar{\phi} = (1/2)\sqrt{r/|u_4|}$; for the second-order transition, $|\bar{\phi}| = \sqrt{|r|/u_4}$ in the ordered phase (see Appendix C). Noticing in both cases that r is linear dependent on the temperature and u_4 is independent of the temperature, we directly get the following scaling laws:

$$\Delta\bar{\phi} \propto (T_{\mathrm{CP}} - T)^{1/2} \text{ and } |\bar{\phi}| \propto (T_c - T)^{1/2}, \tag{5}$$

showing remarkable agreements with the numerical results on these two scalings.

At first sight, this good agreement seems quite unexpected, since due to the fact that long-range fluctuations are neglected in the effective theory within the GL framework it is only expected to provide very rough estimations on the critical exponents for the 2D system under consideration. However, noticing the ILR interaction can strongly suppress the long-range fluctuations [21], this in fact promotes the GL effective theory to a precise effective theory that captures the critical scaling behavior. Such a promotion of the same GL effective theory to a precise effective critical theory is reminiscent of what happens in the 5D Ising model with the same $\mathbb{Z}_2$ symmetry the corresponding scaling exponent of which is exactly 1/2 [22] as in Eq. (5). In the case of the 5D Ising model, the promotion is accomplished via suppressing the

long-range fluctuations by the higher dimensionality, while in contrast it is the long-range interaction that suppresses the long-range fluctuations in lattice Bose gases in cavities. This also indicates its emergent criticality belongs to the 5D Ising universality class, which clearly shows that the criticality of the CDW transition is strongly influenced by the long-range characteristic of the interaction in the system.

V. CONCLUSIONS

The CDW transition of lattice Bose gases in optical cavities is crucially influenced by the thermal fluctuations above the temperature around half the on-site interaction energy: the first-order CDW transition at low temperatures terminates at a critical point where it changes to a second-order phase transition. This gives rise to the new emergent criticality belonging to the 5D Ising universality class, manifesting clearly the long-range characteristic of the system's interaction. Noticing the CDW order parameter can be well measured in current experiments [8], we expect the physics in the emergent critical regime predicted in this paper can be readily observed by operating current experimental setups at a temperature scale around one-half of the on-site energy, or alternatively, by lowering both U_s and U_l in experiments to effectively increase the temperature. Moreover, noticing that even the measurements on the hysteretic behavior hinged to the first-order CDW transition have been already accessible in current experiments [8], identifying the existence of the critical point experimentally can thus be greatly facilitated via monitoring the disappearance of the hysteretic behavior upon increasing temperature from the low-temperature regime. We believe our paper will stimulate further experimental and also theoretical investigations on possible emergent criticalities under the influence of both thermal fluctuations and ILR interactions, especially beyond the deep Mott-insulator limit.

APPENDIX A: EFFECTIVE HAMILTONIAN WITH INFINITE-LONG-RANGE INTERACTIONS

To make the discussion in the main text more self-contained, we present the derivation of the effective Hamiltonian with the ILR interactions shown in Eq. (1), starting from the atom-photon interacting model. Similar derivations with more detailed information concerning the related experiments can be found in Ref. [8]. The physics of lattice bosonic atoms in a 2D square optical lattice within an optical cavity can be captured by the atom-photon interacting model with its Hamiltonian $\hat{H}_{AP}$ assuming the explicit form (units are chosen

such that $\hbar = 1$) [8]

$$\hat{H}_{AP} = \frac{1}{2} \sum_{i,\sigma} U_s \hat{n}_{i,\sigma} (\hat{n}_{i,\sigma} - 1) - t \sum_{\langle (i,\sigma),(j,\sigma') \rangle} (\hat{b}_{i,\sigma}^\dagger \hat{b}_{j,\sigma'} + \text{H.c.})$$
$$+ \lambda (\hat{a}^\dagger + \hat{a})(\hat{N}_e - \hat{N}_o) - (\Delta_c - \delta)\hat{a}^\dagger \hat{a}, \qquad \text{(A1)}$$

where λ is the atom-photon interaction strength, U_s is the strength of the short-range contact interaction between atoms, t is the hopping amplitude, Δ_c is the difference between the frequency of cavity photons and the one of the lattice beam, and δ is a dispersive shift [8]. Here, $\hat{N}_{e(o)} = \sum_{i=1}^{L/2} \hat{n}_{i,e(o)}$ with $\hat{n}_{i,\sigma} \equiv \hat{b}_{i,\sigma}^\dagger \hat{b}_{i,\sigma}$, where $\hat{b}_{i,\sigma}^\dagger (\hat{b}_{i,\sigma})$ is the bosonic creation (annihilation) operator that corresponds to the Wannier function in the lowest band at site i on the sublattice σ. $\hat{a}^\dagger (\hat{a})$ is the creation (annihilation) operator for the photons in the cavity.

To derive the effective Hamiltonian for the atoms only, we first write down the Heisenberg equation of motion for cavity photons with a finite decay rate κ, i.e., $i d\hat{a}/dt = [\hat{a}, \hat{H}_{AP}] - i\kappa \hat{a}$, the explicit form of which reads

$$i \frac{d\hat{a}}{dt} = -(\Delta_c - \delta)\hat{a} - i\kappa \hat{a} + \lambda (\hat{N}_e - \hat{N}_o), \qquad \text{(A2)}$$

where the typical time scale of the dynamics of the cavity photons is determined by the decay rate κ. For the cavity employed in current experiments [6–8], κ is around a few MHz (more precisely, $\kappa = 2\pi \times 1.3$ MHz in experiments reported in [6–8]), which is much larger than the atomic recoil energy E_R, which is usually a few kHz. This indicates the dynamics of the cavity photons are much faster than the ones of atoms. Therefore, one can approximate $\hat{a}$ as

$$\hat{a} = \frac{\lambda (\hat{N}_e - \hat{N}_o)}{\Delta_c - \delta + i\kappa}, \qquad \text{(A3)}$$

and eliminate the cavity photons adiabatically by plugging the above expression into Eq. (A1). After the adiabatic elimination, one obtains the effective Hubbard-type Hamiltonian $\hat{H}_{Hub}$ for the atoms only, i.e.,

$$\hat{H}_{Hub} = -t \sum_{\langle (i,\sigma),(j,\sigma') \rangle} (\hat{b}_{i,\sigma}^\dagger \hat{b}_{j,\sigma'} + \text{H.c.}) \qquad \text{(A4)}$$
$$+ \frac{1}{2} \sum_{i,\sigma} U_s \hat{n}_{i,\sigma} (\hat{n}_{i,\sigma} - 1) - \frac{U_l}{L} (\hat{N}_e - \hat{N}_o)^2,$$

with

$$U_l \equiv -2L\lambda^2 \frac{\Delta_c - \delta}{(\Delta_c - \delta)^2 + \kappa^2}. \qquad \text{(A5)}$$

In the deep Mott-insulator limit, where the hopping amplitude is negligibly small, the system is described by the interaction part of $\hat{H}_{Hub}$ alone, which corresponds to Eq. (1) in the main text.

APPENDIX B: HUBBARD-STRATONOVICH TRANSFORMATION ON THE PARTITION FUNCTION

To investigate finite-temperature properties of the system, the central quantity we need to calculate is the quantum partition function $Z = \text{tr} \exp[-\beta(\hat{H} - \mu\hat{N})]$ with $\hat{N} = \sum_{i,\sigma} \hat{n}_{i,\sigma}$ and μ being the chemical potential. Its explicit form in the

occupation number representation reads

$$Z = \sum_{\{n_{i,\sigma}\}} e^{-\beta\left\{\sum_{i,\sigma}\left[\frac{U_s}{2}n_{i,\sigma}(n_{i,\sigma}-1)-\mu n_{i,\sigma}\right]-\frac{U_l}{L}\left[\sum_i (n_{i,e}-n_{i,o})\right]^2\right\}}, \quad (B1)$$

where $n_{i,\sigma}$ is the occupation number, i.e., the eigenvalue of the bosonic particle number operator $\hat{n}_{i,\sigma}$.

The Hubbard-Stratonovich transformation that we use to introduce the CDW order-parameter field ϕ into the partition function reads

$$\left(\sqrt{\frac{\beta U_l L}{\pi}}\right)^{-1} \exp\left(\beta\frac{U_l}{L}\left[\sum_{i=1}^{L/2}(n_{i,e}-n_{i,o})\right]^2\right) = \int_{-\infty}^{+\infty} d\phi \, \exp\left(-\beta U_l\left\{L\phi^2 + 2\left[\sum_{i=1}^{L/2}(n_{i,e}-n_{i,o})\right]\phi\right\}\right). \quad (B2)$$

By using Eq. (B2) we can replace the long-range interaction term appearing in Eq. (B1) by the integral over the ϕ field and rewrite the partition function Z in terms of ϕ as shown in Eq. (2) in the main text.

ϕ assumes the physical meaning of the fluctuating CDW order-parameter filed. It appears in the partition function and its expectation value $\bar{\phi} \equiv \langle\phi\rangle$ equals to CDW order parameter $\langle\sum_{i=1}^{L/2}\hat{n}_{i,e} - \sum_{i=1}^{L/2}\hat{n}_{i,o}\rangle/L$ exactly. This can be shown by introducing a source J that couples to $L^{-1}\sum_{i=1}^{L/2}(n_{i,e}-n_{i,o})$ in the partition function. Now the partition function depends on the source J and its explicit form reads

$$Z[J] = \sqrt{\frac{\beta U_l L}{\pi}} \int_{-\infty}^{+\infty} d\phi \sum_{\{n_{i,\sigma}\}} e^{-\beta\sum_{i,\sigma}\left[\frac{U_s}{2}n_{i,\sigma}(n_{i,\sigma}-1)-\mu n_{i,\sigma}\right]} e^{-\beta U_l L\phi^2 + 2\beta U_l \phi \sum_{i=1}^{L/2}(n_{i,e}-n_{i,o})} e^{JL^{-1}\sum_{i=1}^{L/2}(n_{i,e}-n_{i,o})}. \quad (B3)$$

One can directly show

$$\frac{\left\langle \sum_{i=1}^{L/2}\hat{n}_{i,e} - \sum_{i=1}^{L/2}\hat{n}_{i,o} \right\rangle}{L} = \left. \frac{\partial \ln Z[J]}{\partial J} \right|_{J=0}. \quad (B4)$$

Moreover, since ϕ is an integral variable with its domain lying in $(-\infty, +\infty)$, one can shift ϕ without changing the partition function. After the shift $\phi \to \phi - \frac{J}{2\beta U_l L}$, we get

$$Z[J] = \sqrt{\frac{\beta U_l L}{\pi}} \int_{-\infty}^{+\infty} d\phi \sum_{\{n_i\}} e^{-\beta\sum_{i,\sigma}\left[\frac{U_s}{2}n_{i,\sigma}(n_{i,\sigma}-1)-\mu n_{i,\sigma}\right]} e^{-\beta U_l L\phi^2 + 2\beta U_l \phi \sum_{i=1}^{L/2}(n_{i,e}-n_{i,o})+\phi J - \frac{J^2}{4\beta U_l L}}. \quad (B5)$$

Now one can calculate the same derivative $\partial \ln Z[J]/\partial J|_{J=0}$ and get

$$\left. \frac{\partial \ln Z[J]}{\partial J} \right|_{J=0} = \langle\phi\rangle. \quad (B6)$$

Comparing Eq. (B4) to Eq. (B6), we conclude ϕ assumes the physical meaning of the fluctuating CDW order-parameter field, with

$$\langle\phi\rangle = L^{-1}\left\langle \sum_{i=1}^{L/2}\hat{n}_{i,e} - \sum_{i=1}^{L/2}\hat{n}_{i,o} \right\rangle. \quad (B7)$$

APPENDIX C: GINZBURG-LANDAU EFFECTIVE THEORY

In the critical regime, the CDW order parameter is small enough to allow a systematic expansion of the system's free energy with respect to its CDW order parameter $\bar{\phi}$. The Ginzburg-Landau free energy F that is allowed by the $\mathbb{Z}_2$ symmetry (i.e., F should be invariant under the transformation $\bar{\phi} \to -\bar{\phi}$) assumes the form

$$F = \frac{1}{2}r\bar{\phi}^2 + \frac{1}{4}u_4\bar{\phi}^4 + \frac{1}{6}u_6\bar{\phi}^6, \quad (C1)$$

where we expand F up to the sixth order in $\bar{\phi}$, with r, u_4, and u_6 being the GL coefficients.

1. Critical scaling of the CDW order-parameter jump $\Delta\bar{\phi}$ in the vicinity of the critical point

To describe the first-order transition, one further assumes that r depends on temperature linearly, i.e., $r = a(T_{\mathrm{CP}} - T)$ where a is a positive coefficient, and $u_{4,6}$ are temperature independent coefficients with $u_4 < 0$ for $T < T_{\mathrm{CP}}$ and u_6 being always positive in order to stabilize the whole system. With $u_4 < 0$, the GL free energy assumes three minima located at

$$\bar{\phi} = 0, \pm\sqrt{\frac{-u_4 + \sqrt{u_4^2 - 4u_6 r}}{2u_6}}, \quad (C2)$$

respectively. For the system parameters located at the first-order transition boundary, the conditions

$$F = 0 \text{ and } \frac{\partial F}{\partial \bar{\phi}} = 0 \quad (C3)$$

should both hold true, from which we can obtain that the nonzero CDW order assumes the values

$$\bar{\phi} = \pm\frac{1}{2}\sqrt{\frac{r}{|u_4|}}. \quad (C4)$$

This thus indicates $\Delta\bar{\phi} = (1/2)\sqrt{r/|u_4|}$. Noticing $r = a(T_{\mathrm{CP}} - T)$ with T being the transition temperature at the first-order transition boundary, this gives rise to the power-law

scaling

$$\Delta\bar{\phi} \propto (T_{\mathrm{CP}} - T)^{1/2}. \tag{C5}$$

2. Critical scaling of the CDW order parameter $\bar{\phi}$ of the second-order CDW transition

Above the critical point, the CDW transition is a second-order phase transition, thus u_4 is assumed to be positive. In this case, the sixth-order term in GL free energy is irrelevant in the vicinity of the transition, therefore we only need to keep up to the fourth-order term in the GL free energy, i.e.,

$$F = \tfrac{1}{2}r\bar{\phi}^2 + \tfrac{1}{4}u_4\bar{\phi}^4. \tag{C6}$$

As the first-order transition case, we assume $r = a(T - T_c)$ with T_c being the critical temperature of the second-order CDW transition. The CDW order is determined by the condition

$$\frac{\partial F}{\partial\bar{\phi}} = 0, \tag{C7}$$

from which we obtain

$$\bar{\phi} = \sqrt{\frac{|r|}{u_4}}, \tag{C8}$$

for $r < 0$. Indeed, noticing $r = a(T - T_c)$, this gives rise to the power scaling

$$\bar{\phi} \propto (T_c - T)^{1/2}. \tag{C9}$$

[1] M. E. Fisher, Rev. Mod. Phys. **46**, 597 (1974).

[2] K. G. Wilson, Rev. Mod. Phys. **47**, 773 (1975).

[3] J. Stuhler, A. Griesmaier, T. Koch, M. Fattori, T. Pfau, S. Giovanazzi, P. Pedri, and L. Santos, Phys. Rev. Lett. **95**, 150406 (2005).

[4] K. K. Ni, S. Ospelkaus, M. H. G. de Miranda, A. Pe'er, B. Neyenhuis, J. J. Zirbel, S. Kotochigova, P. S. Julienne, D. S. Jin, and J. Ye, Science **322**, 231 (2008).

[5] R. Heidemann, U. Raitzsch, V. Bendkowsky, B. Butscher, R. Löw, and T. Pfau, Phys. Rev. Lett. **100**, 033601 (2008).

[6] K. Baumann, C. Guerlin, F. Brennecke, and T. Esslinger, Nature (London) **464**, 1301 (2010).

[7] R. Mottl, F. Brennecke, K. Baumann, R. Landig, T. Donner, and T. Esslinger, Science **336**, 1570 (2012).

[8] R. Landig, L. Hruby, N. Dogra, M. Landini, R. Mottl, T. Donner, and T. Esslinger, Nature (London) **532**, 476 (2016).

[9] H. Ritsch, P. Domokos, F. Brennecke, and T. Esslinger, Rev. Mod. Phys. **85**, 553 (2013).

[10] Y. Li, L. He, and W. Hofstetter, Phys. Rev. A **87**, 051604(R) (2013).

[11] H. Habibian, A. Winter, S. Paganelli, H. Rieger, and G. Morigi, Phys. Rev. Lett. **110**, 075304 (2013).

[12] Y. Chen, Z. Yu, and H. Zhai, Phys. Rev. A **93**, 041601(R) (2016).

[13] N. Dogra, F. Brennecke, S. D. Huber, and T. Donner, Phys. Rev. A **94**, 023632 (2016).

[14] A. E. Niederle, G. Morigi, and H. Rieger, Phys. Rev. A **94**, 033607 (2016).

[15] B. Sundar and E. J. Mueller, Phys. Rev. A **94**, 033631 (2016).

[16] J. Panas, A. Kauch, and K. Byczuk, Phys. Rev. B **95**, 115105 (2017).

[17] R. Liao, H. J. Chen, D. C. Zheng, and Z. G. Huang, Phys. Rev. A **97**, 013624 (2018).

[18] Critical scaling behavior belonging to the mean-field universality class (the 5D Ising universality class is a mean-field universality class) can indeed match experimental observations reasonably well in a few cases, for instance, transitions between normal metals and conventional superconductors, order-disorder transitions in liquid crystals, and ferroelectric-paramagnetic transitions. However, this is due to the fact that according to the Ginzburg criterion [19] the real critical region in these cases, for instance, the temperature region around the transition, where scaling behavior beyond the mean-field ones manifest, is too small to be accessed in experiments.

[19] V. L. Ginzburg, Sov. Phys. Solid State **2**, 1824 (1960).

[20] M. Kac, G. E. Uhlenbeck, and P. C. Hemmer, J. Math. Phys. **4**, 216 (1963).

[21] F. Bouchet, S. Gupta, and D. Mukamel, Physica A **389**, 4389 (2010).

[22] M. Aizenman, Phys. Rev. Lett. **47**, 1 (1981).